BIOCHEMICAL PHARMACOLOGY 76 (2008) 1705–1715

available at www.sciencedirect.com

ScienceDirect

journal homepage: www.elsevier.com/locate/biochempharm

Glibenclamide exerts an antitumor activity through reactive oxygen species–c-jun NH(2)-terminal kinase pathway in human gastric cancer cell line MGC-803

Xia Qian, Jing Li, Jianhua Ding, Zhiyuan Wang, Lei Duan, Gang Hu *

Department of Pharmacology, Nanjing Medical University, 140 Hanzhong Road, Nanjing, Jiangsu 210029, PR China

ARTICLE INFO

Article history:
Received 29 July 2008
Accepted 5 September 2008

Keywords:
Glibenclamide
Human gastric cancer cell line
MGC-803
Reactive oxygen species
C-jun NH(2)-terminal kinase
Akt

ABSTRACT

Glibenclamide, a blocker of ATP-sensitive potassium (K_{ATP}) channels, can suppress progression of many cancers, but the involved mechanism is unclear. Herein we reported that MGC-803 cells expressed the K_{ATP} channels composed of Kir6.2 and SUR1 subunits. Glibenclamide induced cellular viability decline, coupled with cell apoptosis and reactive oxygen species (ROS) generation in MGC-803 cells. Meanwhile, glibenclamide increased NADPH oxidase catalytic subunit $gp91^{phox}$ expression and superoxide anion (O_2^-) generation, and caused mitochondrial respiration dysfunction in MGC-803 cells, suggesting that glibenclamide induced an increase of ROS derived from NADPH oxidase and mitochondria. Glibenclamide could also lead to loss of mitochondrial membrane potential, release of cytochrome c and apoptosis-inducing factor (AIF), and activation of c-jun NH(2)-terminal kinase (JNK) in MGC-803 cells. Pretreatment with antioxidant N-acetyl-L-cysteine (NAC) prevented glibenclamide-induced JNK activation, apoptosis and cellular viability decline. Furthermore, glibenclamide greatly decreased the cellular viability, induced apoptosis and inhibited Akt activation in wild-type mouse embryonic fibroblast (MEF) cells but not in $JNK1^{-/-}$ or $JNK2^{-/-}$ MEF cells. Taken together, our study reveals that glibenclamide exerts an antitumor activity in MGC-803 cells by activating ROS-dependent, JNK-driven cell apoptosis. These findings provide insights into the use of glibenclamide in the treatment of human gastric cancer.

1. Introduction

ATP-sensitive potassium (K_{ATP}) channels that are gated by intracellular ATP/ADP concentrations play essential roles in coupling cell metabolic events to electrical activity [1]. The K_{ATP} channel located in surface membrane (surfaceK_{ATP} channel) or in the mitochondrial inner membrane (mitoK_{ATP} channel) is an octamer, formed by the physical association of four inwardly rectifying potassium channel subunits (Kir6.*x*) and four regulatory sulfonylurea receptor subunits (SUR) [2]. The exact subunit composition differs among different tissues, including pancreas, cardiac, smooth and skeletal muscle and brain [2]. Recently, it was demonstrated that opening of K_{ATP} channels especially mitoK_{ATP} channels inhibited apoptosis in ischemia, hypoxia or oxidative stress-induced injury by promoting ATP synthesis, attenuating Ca^{2+} accumulation, regulating the generation of ROS and its downstream PKC, MAPK signaling pathways, enhancing

* *Corresponding author*. Tel.: +86 25 86863169; fax: +86 25 86863108.
E-mail address: ghu@njmu.edu.cn (G. Hu).

Abbreviations: K_{ATP}, ATP-sensitive potassium channels; ROS, reactive oxygen species; RCR, respiratory control ratio; AIF, apoptosis-inducing factor; JNK, c-jun NH(2)-terminal kinase; NAC, N-acetyl-L-cysteine; $\Delta\Psi m$, mitochondrial membrane potential.

0006-2952/$ – see front matter © 2008 Elsevier Inc. All rights reserved.
doi:10.1016/j.bcp.2008.09.009

Bcl-2 expression, and inhibiting the release of cytochrome c from mitochondria, and these effects could be reversed by blockers of K_{ATP} channels [3,4]. Also, K_{ATP} channel openers (minoxidil, cromakalim and pinacidil) were reported to increase HepG2 cell proliferation, whereas K_{ATP} channel blockers (quinidine and glibenclamide) attenuated HepG2 cell proliferation [5], and glibenclamide could inhibit progression of many cancers such as bladder carcinoma [6], prostate cancer [7], liver cancer [5]. However, the molecular mechanisms for the anticancer actions of glibenclamide remain to be elucidated.

Reactive oxygen species (ROS) including superoxide (O_2^-), hydroxyl radical ($^{\bullet}OH$) and H_2O_2 are generated in a variety of cells stimulated with cytokines, peptide growth factors, irradiations or inflammatory system [8]. NADPH oxidase and mitochondria are two major sources of ROS [9]. Electrons from NADPH are transferred through the enzyme to molecular oxygen to generate superoxide, with the secondary production of other ROS [10]. Embedded in the lipid bilayer of the mitochondrial inner membrane, the oxidative phosphorylation system (OXPHOS) is another ROS production pathway, and the retardation of mitochondrial respiratory chain promotes the generation of ROS [11]. ROS at low concentration functions as a physiological mediator in many cellular events, including cell proliferation, glucose transport and lipid synthesis, while excessive ROS production causes direct cellular damage and induces cell death [12]. ROS can activate several mitogen-activated protein serine/threonine kinases (MAPKs), which transduce diverse extracellular stimuli (mitogenic growth factors, environmental stresses, and proapoptotic agents) to the nucleus via kinase cascades to regulate a wide array of cellular processes, including proliferation, differentiation and apoptosis [13]. It has been demonstrated that many cancer chemotherapeutic agents can be selectively toxic to tumor cells by inducing production of ROS, loss of mitochondrial membrane potential, and activation of mitochondrial apoptosis pathways [14–16]. Therefore, ROS has been an important target for developing antitumor drugs.

In the present study, we first investigated whether K_{ATP} channels are expressed in MGC-803 cells and whether their blocker glibenclamide exerts anticancer activity. Then, the mechanisms underlying the anticancer effects of glibenclamide on MGC-803 cells were further explored. The results show that glibenclamide induced apoptosis of MGC-803 cells by activating mitochondrial death pathways related to the generation of ROS, activation of JNK and inhibition of Akt pathway. These findings provide crucial evidence and molecular insight for the use of glibenclamide in the treatment of human gastric cancer.

2. Materials and methods

2.1. Materials and reagents

Glibenclamide was purchased from Tocris, dissolved at 10 mM concentration in dimethylsulfoxide (DMSO; Sigma) and kept as stock solutions. NAC, MTT and Hoechst 33342 were purchased from Sigma (St Louis, MO, USA). DMEM and fetal bovine serum (FBS) were purchased from Life Technologies, Inc. Antibodies against Kir6.1, Kir6.2, SUR1 and SUR2 were purchased from Santa Cruz Biotechnology, Inc., and the antibodies against phosphorylated Akt (Ser473), Akt, phosphorylated JNK, JNK, Cytochrome c and AIF were from Cell Signaling Technology, Inc.

2.2. Cell culture

Human gastric cancer cell line MGC-803 was supplied by the Cell Bank of Shanghai Institute of Cell Biology. Wild type, $JNK1^{-/-}$, and $JNK2^{-/-}$ mouse embryonic fibroblast (MEF) cells were presented as a gift by Prof. Y. Wan (Department of Biology, Providence College). These cells were cultured in DMEM containing 10% fetal calf serum, 100 U/ml penicillin and 100 μg/ml streptomycin, and maintained in a humidified atmosphere of 95% air and 5% CO_2 at 37 °C.

2.3. Cell viability assay

Cell viability was measured by MTT method. The absorbance of each well was obtained using a Dynatech MR5000 plate counter at a test wavelength of 570 nm with a reference wavelength of 630 nm. The following formula was used to calculate cell viability: percentage cell viability = (absorbance of the experiment samples/absorbance of the control) × 100.

2.4. Hoechst 33342 staining

To quantify apoptotic cells, cellular monolayer was fixed and stained with Hoechst 33324. The morphological features of apoptosis (cell shrinkage, chromatin condensation, and fragmentation) were monitored by fluorescence microscopy (Olympus BX 60, Tokyo, Japan). At least 400 cells from 12 randomly selected fields per dish were counted, and each treatment was performed in triplicate.

2.5. Reverse transcription-polymerase chain reaction (RT-PCR)

Total RNA was extracted from MGC-803 cells after stimulation using Trizol (Invitrogen Life technologies, USA). Total RNA (2 μg) from MGC-803 cells was reversely transcribed into single-stranded cDNA. PCR was performed on the equivalent cDNAs from each sample. Amplification was performed with specific sets of primers: $gp91^{phox}$ (forward 5′-TGACTCGGTTGGCTGGCATC-3′ and reverse 5′-CGCAAAGGTACAGGAACATGGG-3′), and glyceraldehyde-3-phosphate dehy-drogenase (GAPDH) was used as housekeeping gene (forward 5′-TGGT GCCAAAAGGGTCATCTCC-3′ and reverse 5′-GCCAGCCCCAGCATCAAAGGTG-3′). PCR cycles were as follows: $gp91^{phox}$ and GAPDH: 94 °C, 4 min; 94 °C, 30 s; 60 °C, 30 s; 72 °C, 30 s; 72 °C, 5 min (32 cycles). The PCR reactions were then visualized on a 1.8% agarose gel containing 0.06 μg/ml ethidium bromide and the resulting bands were confirmed using Molecular Image FX (BIO-RAD).

2.6. Measurement of ROS

Formation of ROS was evaluated using 2′, 7′-dichlorofluorescein diacetate (DCFH-DA; Sigma). DCFH-DA enters cells passively and is de-acetylated by esterase to non-fluorescent

DCFH. DCFH reacts with ROS to form DCF, the fluorescent product. DCFH-DA was dissolved in ethanol at 10 mM and was diluted 500-fold in DMEM to give DCFH-DA at 20 μM. Cells were exposed to DCFH-DA for 1 h and then treated with DMEM containing corresponding concentration of glibenclamide for 3 h. The fluorescence was visualized immediately at wavelengths of 485 nm for excitation and 530 nm for emission by a Nikon Optical TE2000-S (Tokyo, Japan) inverted fluorescence microscope. And the total green fluorescence intensities of every well were quantitated using image-analysis software (Simple PCI, Hamamatsu City, Japan).

2.7. Superoxide production

Superoxide ions were detected using dihydroethidium (DHE, Molecular Probes, Eugene, OR, USA). DHE is a cell-permeable fluorescent dye that is oxidized to generate two fluorescent products, 2-hydroxyethidium (EOH) and ethidium [17]. The fluorescence intensity indicates the relative level of superoxide production [18]. MGC-803 cells were treated with DMEM containing corresponding concentration of glibenclamide for 3 h. Then, the cells were incubated with 2 μM DHE for 30 min. The cells were then washed and examined with a Nikon Optical TE2000-S inverted fluorescence microscope at wavelengths of 535 nm for excitation and 610 nm for emission. And the total red fluorescence intensities of every well were quantitated using image-analysis software.

2.8. Isolation of mitochondria

Mitochondria were isolated by using a differential centrifugation method (500, 800, 1000 × *g*) that retains mitochondrial structure and respiratory functions [19]. MGC-803 cells ($2.5–5 \times 10^8$) were harvested and placed on ice for 15 min, centrifuged at 500 × *g* for 5 min at 4 °C, washed one time with ice-cold PBS, and subsequently washed with ice-cold mitochondrial isolation buffer (MIB) (200 mM mannitol, 70 mM sucrose, 1 mM EGTA, 10 mM Hepes; pH 7.4). MGC-803 cells were resuspended in ice-cold MIB + 0.5 mg/ml BSA (MIB/BSA) and then homogenized in a syringe-driven cell disruptor. The lysate was spun at 800 × *g* for 10 min at 4 °C. Supernatants were removed and spun at 10,000 × *g* for 10 min at 4 °C. Pellets were resuspended in MIB/BSA and normalized by protein concentration. Mitochondrial protein concentration was quantified according to Bradford [20] using BSA as standard, and the mitochondria were diluted in isolation buffer to yield a fixed concentration before measurement.

2.9. Mitochondrial respiration

Respiratory activities of mitochondrial preparations were measured by determining oxygen consumption using a Clark Electrode provided by Hansatech (King's Lynn, UK). The incubation medium was constantly stirred using an electromagnetic stirrer and bar flea. The oxygen consumption studies were conducted at 30 °C in respiration medium consisting of 25 mM sucrose, 75 mM mannitol, 95 mM KCl, 5 mM KH_2PO_4, 20 mM Tris–HCl, 1 mM EGTA, pH 7.4. The concentrations of substrates used were 5 mM glutamate and 5 mM malate, which were added to the respiration media before the mitochondria. Approximately 0.5 mg of mitochondrial protein was preincubated in the oxygen electrode in a total volume of 1 ml with substrates for 5 min before the addition of reagents to give a final concentration of 5–100 μM glibenclamide and the vehicle of 100 μM glibenclamide. The mitochondrial suspension was incubated for 2 min in the oxygen electrode to allow for reagents uptake. State 3 respiration (ST3) was induced by the addition of ADP (1 mM). Approximately 3 min later, ST3 was terminated and state 4 respiration (ST4) (resting) was detected. The respiratory control ratio (RCR) was calculated from the ratio of the ST3/ST4 oxygen consumption rates, with and without ADP, respectively [21].

2.10. Measurement of MGC-803 cell mitochondrial membrane potential ($\Delta\Psi m$)

MGC-803 cell mitochondrial membrane potential was assessed with the fluorescent probe JC-1 (Molecular Probes, Eugene, OR, USA). At 490 nm, cells with polarized mitochondria predominantly contained JC-1 in aggregate form, and mitochondria fluoresced red–orange. Cells with depolarized mitochondria contained JC-1 predominantly in monomeric form and fluoresced green. Cells were incubated with 5 μM JC-1 for 10 min at 37 °C, washed, and placed on a thermostatted stage at 37 °C. Fluorescent images were visualized by a Nikon Optical TE2000-S inverted fluorescence microscope with excitation at 490 nm and emission at 520 nm. MGC-803 cells with polarized mitochondria were seen with distinct mitochondria fluorescing red-orange, and, in MGC-803 cells with depolarized mitochondria, the cytoplasm and mitochondria appeared green. Acquired signal was analyzed with image-analysis software. A minimum of six fields were selected and average intensity for each region was quantified. The ratio of J-aggregate to JC-1 monomer intensity for each region was calculated. A decrease in this ratio was interpreted as loss of $\Delta\Psi m$, whereas an increase in the ratio was interpreted as gain in $\Delta\Psi m$.

2.11. Western blot analysis

After drug treatment, cells were washed twice with ice-cold PBS and homogenized in 200 μl lysis buffer. After incubation for 20 min on ice, cell lysates were centrifuged (10,000 × *g* for 10 min at 4 °C) and protein concentration in the extracts was determined by the Bradford assay. Proteins in cell extracts were denatured with SDS sample buffer and separated by 10% SDS-PAGE. Proteins were transferred to nitrocellulose membranes using a Bio-Rad miniprotein-III wet transfer unit. Nonspecific binding was blocked with 5% nonfat milk dissolved in TBST (pH 7.5, 10 mM Tris–HCl, 150 mM NaCl, and 0.1% Tween-20) for 1 h at room temperature. The membranes were then incubated overnight at 4 °C with individual primary antibodies including antibodies against different subunits of K_{ATP} channel (Kir6.1, Kir6.2, SUR1 and SUR2), anti-JNK, anti-phospho-JNK, anti-Akt, and anti-phospho-Akt. Following three washes with TBST, the membranes were then incubated with the horseradish peroxidase-conjugated secondary antibodies dilution in TBST containing 5% BSA for 1 h at room temperature. The membranes were then washed thrice with TBST and the protein bands were

visualized with the ECL Western blotting detection system according to the manufacturer's instructions.

For mitochondrial cytochrome c and AIF Western blot analysis, mitochondrial proteins (50 μg) isolated from MGC-803 cells after glibenclamide treatment were subjected to Western blot analysis using a monoclonal cytochrome c and AIF antibody.

2.12. Statistical analysis

Statistical analysis was done using two-tailed Student's *t*-test. All values were expressed as mean ± S.D. of triplicate samples. Differences were considered significant at $P < 0.05$.

3. Results

3.1. MGC-803 cells express K_{ATP} channel subunits Kir6.2 and SUR1 but not Kir6.1 and SUR2

Initial experiments were undertaken to detect the expression of K_{ATP} channel subunits in MGC-803 cells. The results of Western blot analysis showed that prominent bands at expected molecular weights of 50 kDa for Kir6.2 and 150 kDa for SUR1 were observed in MGC-803 cells. However, no obvious bands at expected molecular weights of 50 kDa for Kir6.1, 130 kDa and 30 kDa for SUR2 were detected (Fig. 1A). These results indicate that MGC-803 cells express the K_{ATP} channels composed of Kir6.2 and SUR1 subunits.

3.2. Glibenclamide decreases the viability and induces apoptosis of MGC-803 cells

Incubation of MGC-803 cells with glibenclamide for 48 h resulted in a concentration-dependent reduction of cell viability (Fig. 1B). This result indicates that glibenclamide exerts antitumor activity in MGC-803 cells.

The nuclear staining with Hoechst 33342 was performed on MGC-803 cells so as to investigate whether the antitumor activity exerted by glibenclamide involved cellular apoptosis. As shown in Fig. 1C, untreated MGC-803 cells exhibited regular and round shaped nuclei. In contrast, the condensation and fragmentation of nuclei, the characteristic of apoptotic cells, were evident in the cells treated with different concentrations of glibenclamide for 48 h, suggesting that glibenclamide treatment induced apoptosis of MGC-803 cells.

3.3. Glibenclamide induces ROS generation in MGC-803 cells

K_{ATP} channels have been reported to regulate the ROS generation [3,4], and ROS functions as a pivotal component in a proapoptotic signaling cascade [22]. We therefore hypothesized that glibenclamide may affect cellular ROS generation. To test this hypothesis, we monitored ROS levels using a fluorescent probe, DCFH-DA, which is nonfluorescent until it is oxidized by ROS within the cell. The representative fluorescent microscopic images in Fig. 2A showed that the treatment with glibenclamide (5, 50 and 100 μM) induced an increase in DCFH-DA fluorescence within 3 h in a concentration-dependent manner, while the vehicle of glibenclamide 100 μM significantly decreased ROS production. These data support our hypothesis that glibenclamide treatment leads to an increase in ROS production, which may represent a critical step in glibenclamide-induced apoptosis in MGC-803 cells.

NADPH oxidase is one of the major sources of ROS, and its activation produces superoxide ions that are subsequently converted to hydrogen peroxide (H_2O_2) by superoxide dismutase (SOD) [23]. Analysis of superoxide anion (O_2^-) generation with fluorescent dye DHE can assess NADPH oxidase activity [17]. Recent studies indicated that DHE is susceptible to nonspecific oxidation by two electrons to generate ethidium, or selective oxidation by O_2^- to generate 2-hydroxyethidium (2-OH-E$^+$). However, the fluorogenic probe DHE remains the probe of choice to detect and quantify the O_2^- in cellular systems [24]. We used DHE to detect glibenclamide treatment-induced O_2^- generation. As shown in Fig. 2B, treatment of MGC-803 with glibenclamide (5, 50, 100 μM) for 3 h significantly increased O_2^- generation, and RT-PCR analysis showed that glibenclamide increased the expression of NADPH oxidase catalytic subunit gp91^{phox} in a concentration-dependent manner within 1 h. Although glibenclamide 100 μM vehicle can also increase gp91^{phox} mRNA levels, the effect of glibenclamide 100 μM is much greater than its vehicle. These results suggest that glibenclamide can induce ROS production through activation of NADPH oxidase.

It has been documented that the retardation of mitochondrial respiratory chain can promote ROS generation [11]. So the mitochondria prepared from MGC-803 cells were used to investigate the effect of glibenclamide on mitochondrial respiratory. The RCR ratio (state 3/state 4) provides a measure of mitochondrial integrity and is a sign of the compactness of coupling mitochondria [25]. The result showed that incubation with glibenclamide (100 μM) induced a significant decrease in respiratory control ratio (RCR) (Fig. 2C), indicative of the retardation of mitochondrial respiratory chain. We conclude that glibenclamide treatment results in an increase of ROS derived from both NADPH oxidase and mitochondria of MGC-803 cells.

To further determine whether glibenclamide treatment-induced increase of ROS is involved in its antitumor effect, we tested the effect of antioxidant NAC on the changes of MGC-803 cell viability and apoptosis induced by glibenclamide (100 μM) after 48 h of treatment. It was found that pretreatment with NAC (1 mM) for 1 h abrogated glibenclamide-induced viability decline and apoptosis of MGC-803 cells (Fig. 2D). These findings indicate that ROS production increased by glibenclamide may be a requirement in glibenclamide-induced apoptosis in MGC-803 cells.

3.4. Glibenclamide leads to loss of mitochondrial membrane potential and release of pro-apoptotic factors from mitochondria of MGC-803 cells

ROS can initiate apoptosis via the mitochondrial pathway by inducing loss of the mitochondrial membrane potential ($\Delta\Psi m$), and release of mitochondrial pro-apoptotic proteins such as cytochrome c and AIF [26]. In the present study, JC-1 staining showed that glibenclamide (50 μM) treatment for 3, 12, and 24 h resulted in a loss of $\Delta\Psi m$ in a time-dependent

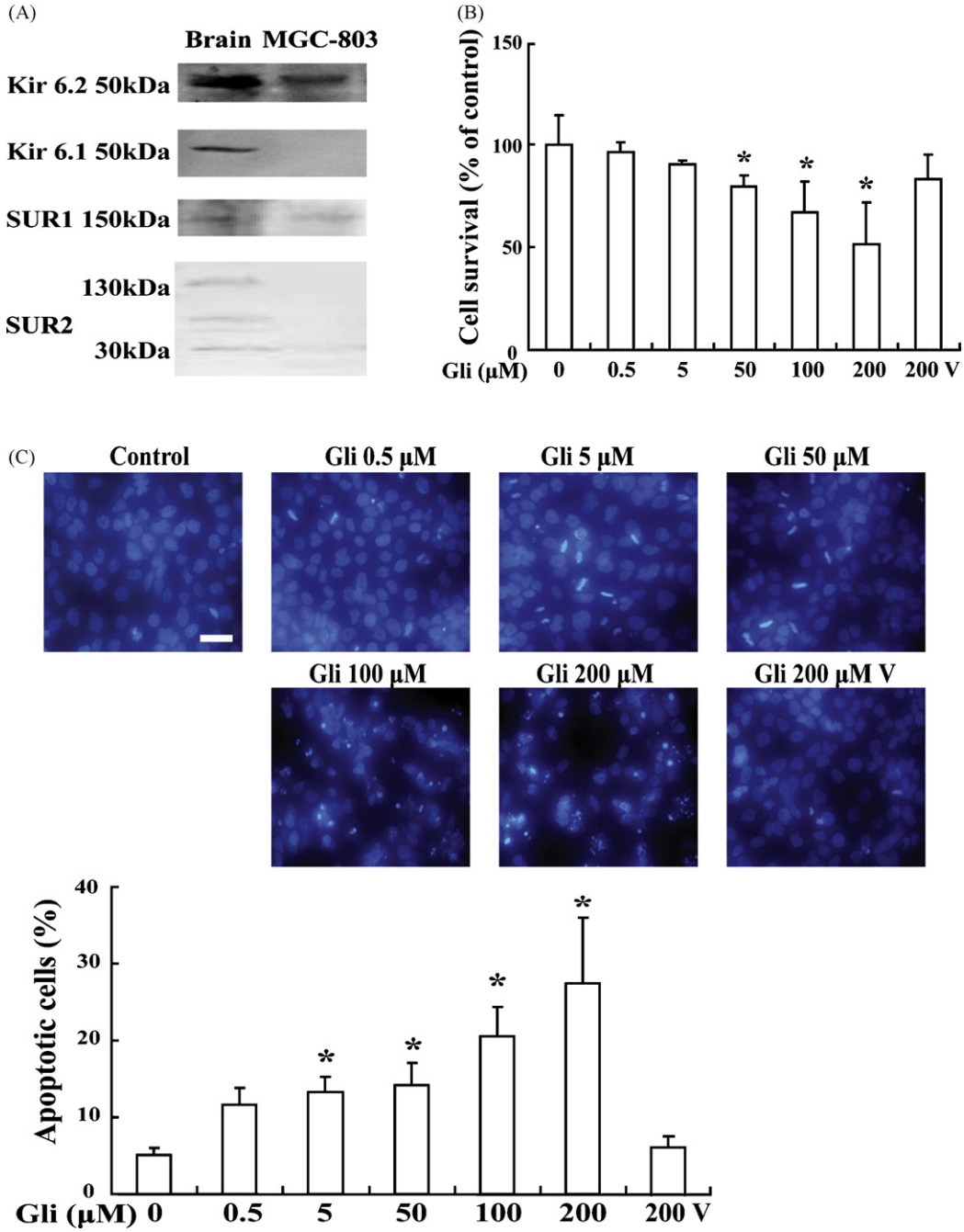

Fig. 1 – Effects of glibenclamide on the viability and apoptosis of MGC-803 cells. (A) Western blot analysis of Kir6.2 and SUR1 subunits expression in MGC-803 cells. The brain tissue (Brain) was used as positive control of Kir6.2, Kir6.1, SUR1 and SUR2. (B) MTT assay showed that glibenclamide (Gli) decreased the viability of MGC-803 cells in a concentration-dependent manner after treatment for 48 h, and the vehicle of 200 μM glibenclamide (Gli 200 V) had no effect on the viability of these cells. (C) Fluorescence microscopy images of Hoechst 33342-stained cells showing the appearance of apoptotic morphology in glibenclamide treated MGC-803 cells in a concentration-dependent manner. Scale bar: 50 μm. Lower histogram: quantitative analysis of % condensed nucleus as in above fluorescence images. Columns, mean of triplicates from three separate experiments; bars, S.D. *P* represents statistical analysis. $^{*}P < 0.05$, vs. control group.

manner, with a maximum effect at 24 h (data not shown). Furthermore, glibenclamide (5, 50 and 100 μM) caused loss of $\Delta\Psi m$ after 24 h of treatment in a concentration-dependent manner (Fig. 3A). Western blot analysis revealed that the mitochondrial levels of cytochrome c and AIF were decreased in the MGC-803 cells treated with glibenclamide for 24 h (Fig. 3B and C). These results implied that glibenclamide increased the release of cytochrome c and AIF from mitochondria and subsequently increased the cytosolic cytochrome c levels and nuclear AIF levels, and eventually triggered the

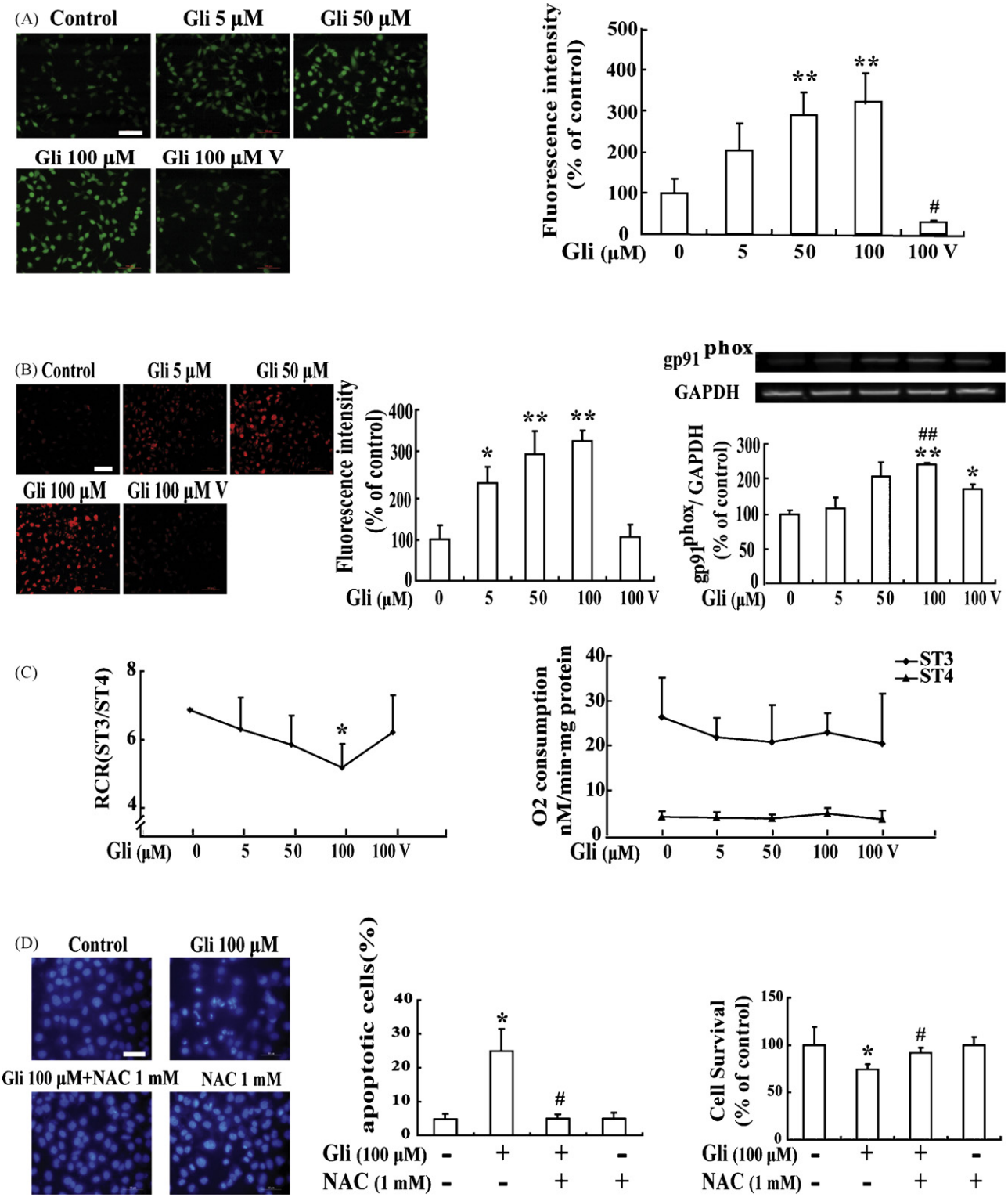

Fig. 2 – Glibenclamide induces production of ROS in MGC-803 cells. (A) DCFH-DA fluorescence (green) imaging of ROS in MGC-803 cells. Cells were labeled with DCFH-DA 10 μM and then treated with indicated concentration of glibenclamide for 3 h. Scale bar: 100 μm. (B) Effects of glibenclamide on NADPH oxidase activity. MGC-803 cells were treated with indicated concentration of glibenclamide for 3 h and then labeled with DHE 2 μM for 30 min, the O_2^- levels were indicated by the red fluorescence intensities. Scale bar: 100 μm. MGC-803 cells were treated with indicated concentration of glibenclamide for 3 h and then the total RNA was extracted and RT-PCR was performed to analysis the expression of $gp91^{phox}$. (C) Effects of glibenclamide on mitochondrial respiration of MGC-803 cells. Freshly isolated MGC-803 mitochondria (0.5 mg) in 1 ml of the standard medium were incubated with indicated concentration of glibenclamide for 2 min. Respiratory activities of mitochondrial preparations were measured by determining oxygen consumption as described in Section 2. (D) Antioxidant

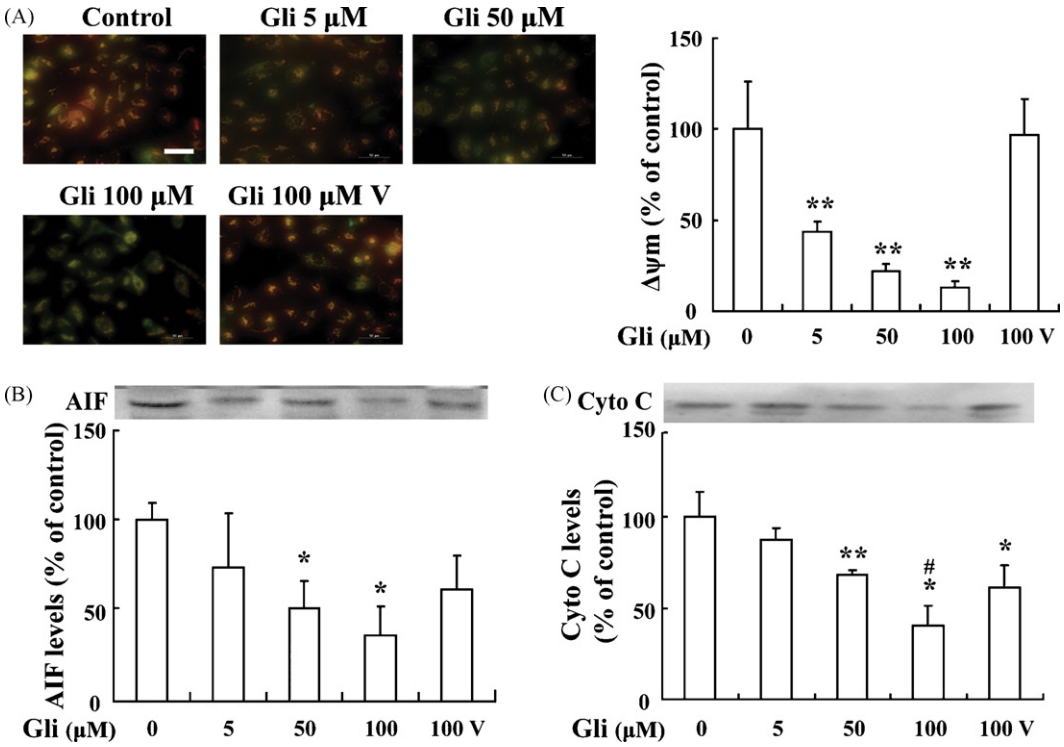

Fig. 3 – Glibenclamide activates mitochondria apoptosis pathways. (A) JC-1 fluorescence imaging of mitochondria. After the application of glibenclamide for 24 h, JC-1 fluorescence shifted from red-orange to green, which indicated the depolarization of mitochondrial membrane potential. Quantification of mitochondrial membrane potential expressed as a ratio of J-aggregate to JC-1 monomer (red:green) fluorescence intensity. Scale bar: 50 μm. (B, C) Cells were incubated with indicated concentrations of glibenclamide for 24 h. Then, mitochondrial extracts (50 μg) were obtained and analyzed with anti-AIF (B) or anti-cytochrome c antibodies (C) by Western blot. Although glibenclamide 100 μM vehicle (Gli 100 V) can also induce cytochrome c release from mitochondria, the effect of glibenclamide 100 μM is much greater than its vehicle. $^{*}P < 0.05$ vs. control group; $^{**}P < 0.01$ vs. control group; $^{\#}P < 0.05$ vs. vehicle group. (For interpretation of the references to color in this figure legend, the reader is referred to the web version of the article.)

caspase-dependent and caspase-independent apoptosis pathway, respectively.

3.5. *Glibenclamide induces activation of JNK as a downstream event of ROS production*

An increase in ROS is also associated with the activation of the redox sensitive JNK signaling pathway [27–29]. To investigate whether glibenclamide-induced ROS leads to the activation of JNK in MGC-803 cells, we determined the phosphorylation state of JNK in MGC-803 cells treated with glibenclamide. As shown in Fig. 4A, glibenclamide (50,100 μM) treatment for 24 h significantly increased the phosphorylation of JNK. Furthermore, pretreatment with NAC (1 mM) for 1 h could prevent the phosphorylation of JNK caused by glibenclamide (100 μM) (Fig. 4B). These results indicate that ROS production induced by glibenclamide contributes to the activation of JNK.

3.6. *The antitumor activity of glibenclamide is suppressed in JNK1$^{-/-}$ or JNK2$^{-/-}$ MEF cells*

Increasing evidence shows that JNK plays an important role in apoptosis by directly initiating mitochondrial death pathways [30] or indirectly inhibiting Akt anti-apoptotic signaling pathway [31]. In the present study, JNK1$^{-/-}$ or JNK2$^{-/-}$ MEF cells were used to determine whether JNK is required for glibenclamide-induced apoptosis. As shown in Fig. 5A and B, glibenclamide markedly decreased the cellular viability and induced apoptosis in wild-type MEF cells but not in JNK1$^{-/-}$ or JNK2$^{-/-}$ MEF cells. Notably, glibenclamide treatment resulted in a significant reduction of phospho-Akt levels in wild-type

(NAC) inhibited the antitumor effect of glibenclamide. Fluorescence microscopy images of Hoechst 33342-stained cells showed that pretreatment with NAC (1 mM) for 1 h suppressed glibenclamide (100 μM) treatment-induced apoptosis of MGC-803 cells. MTT assay showed pretreatment with NAC inhibited glibenclamide-induced cell viability decline. $^{*}P < 0.05$ vs. control group; $^{**}P < 0.01$ vs. control group; $^{\#}P < 0.05$ vs. control group; $^{\#\#}P < 0.01$ vs. vehicle group. (For interpretation of the references to color in this figure legend, the reader is referred to the web version of the article.)

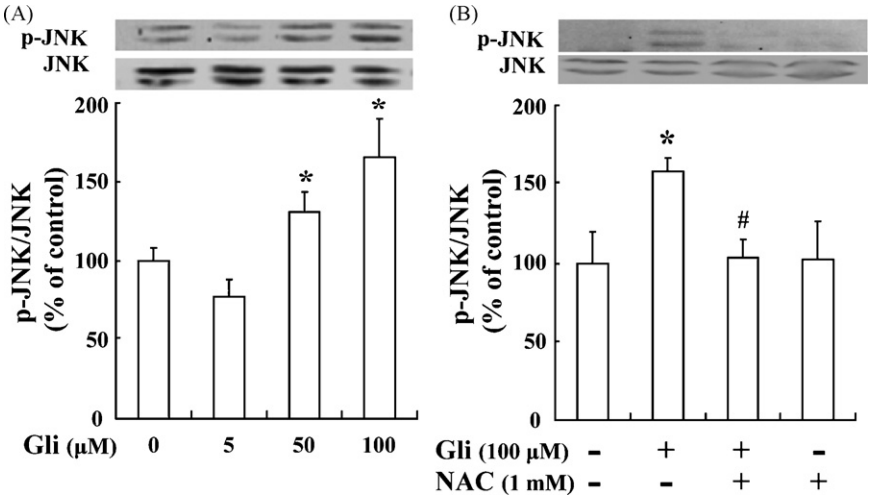

Fig. 4 – Effects of glibenclamide on JNK activity. (A) Cells were incubated with indicated concentrations of glibenclamide for 24 h, and then, cell proteins were obtained and analyzed with antiphospho-JNK and anti-JNK antibodies by Western blot. Glibenclamide (50, 100 μM) significantly increased the phosphorylation of JNK. (B) Pretreatment with NAC (1 mM) for 1 h suppressed glibenclamide (100 μM)-induced JNK phosphorylation. Upper: representative blots are shown. Lower: densitometric analysis of the phosphorylated forms of JNK. $^{*}P < 0.05$ vs. control group. $^{\#}P < 0.05$ vs. glibenclamide treatment group.

MEF cells but not in the JNK1$^{-/-}$ or JNK2$^{-/-}$ MEF cells (Fig. 5C). These data strongly indicate a critical role for JNK activation in the antitumor activity of glibenclamide.

4. Discussion

Cancer drug therapy is undergoing a major transition from a previous ''cytotoxic'' era to a new ''post-genomic'' era, where mechanism-based therapeutic agents will be designed to act on molecular targets that are involved in the malignant progression of human cancers [32]. Accumulated evidence suggests that K^+ channels are potential targets for cancer therapy [32–34]. The K_{ATP} channel is one member of inwardly rectifying K^+ (Kir) channels and influenced by the ATP/ADP ratio [35]. In responding to cytoplasmic nucleotide levels, K_{ATP} channel activity provides a unique link between cellular energetics and electrical excitability [36]. Abundant studies have demonstrated that opening of K_{ATP} channels protected cells against apoptosis in ischemia, hypoxia and oxidative stress-induced injury, while closing of K_{ATP} channels enhanced cell damage and promoted cell apoptosis [3,4]. The present study demonstrated that MGC-803 cells expressed the K_{ATP} channels composed of Kir6.2 and SUR1 subunits. Thus, it is highly likely that closure of K_{ATP} channels in MGC-803 may exert an anticancer effect through initiating apoptotic pathways.

Glibenclamide, a K_{ATP} channel blocker, can close K_{ATP} channels, leading to membrane depolarization, opening of voltage-gated Ca^{2+} channels, Ca^{2+} influx, rise in cytoplasmic free calcium concentration ($[Ca^{2+}]_i$), and thereby exocytosis of insulin granules, and therefore it has been used in the therapy of type 2 diabetes [37]. The results in the present study suggested that glibenclamide exerted a significant antitumor activity, as shown by the potent cell apoptosis and suppressed cell viability of MGC-803 cells, which was consistent with previous reports that closure of K_{ATP} channels with glibenclamide markedly reduced cell proliferation in liver cancers [5] and induced cell apoptosis in human bladder and prostate cancer cells [6,7]. However, the detailed mechanisms by which glibenclamide exerts antitumor activity are still unclear. Our data show that glibenclamide-increased ROS generation is an early event that activates JNK and subsequently triggers the mitochondrial apoptotic pathways.

ROS is generated by all aerobic organisms and it seems to be indispensable for signal transduction pathways that regulate cell growth and reduction–oxidation (redox) status [38]. However, overproduction of these highly reactive oxygen metabolites can initiate lethal chain reactions, which involve oxidation and damage to the structures that are crucial for cellular integrity and survival [39]. Emerging evidence suggests that most cancer cells are under oxidative stress associated with increased metabolic activity and production of ROS, making them vulnerable to chemotherapeutic agents that further augment ROS generation or weaken the antioxidant defenses of the cells [40]. Notably, glibenclamide induced apoptosis concomitant with increased ROS generation in MGC-803 cells, indicating that glibenclamide may exert anticancer activity by increasing the production of ROS. This assumption is strongly supported by the results that the antioxidant NAC could effectively block glibenclamide-induced apoptosis and cellular viability decline in MGC-803 cells. ROS may originate from the cytosolic NADPH oxidase and mitochondria in the cancer cells [9]. It has been reported that ROS derived from NADPH oxidases is correlated with the induction of apoptosis [9]. The NADPH oxidase consists of the catalytic subunit $gp91^{phox}$ (otherwise known as NOX2), together with the regulatory subunits $p22^{phox}$, $p47^{phox}$, $p40^{phox}$, $p67^{phox}$ and the small GTPase Rac [10]. Gp91phox is the limiting subunit of NADPH oxidase, and the increase of its

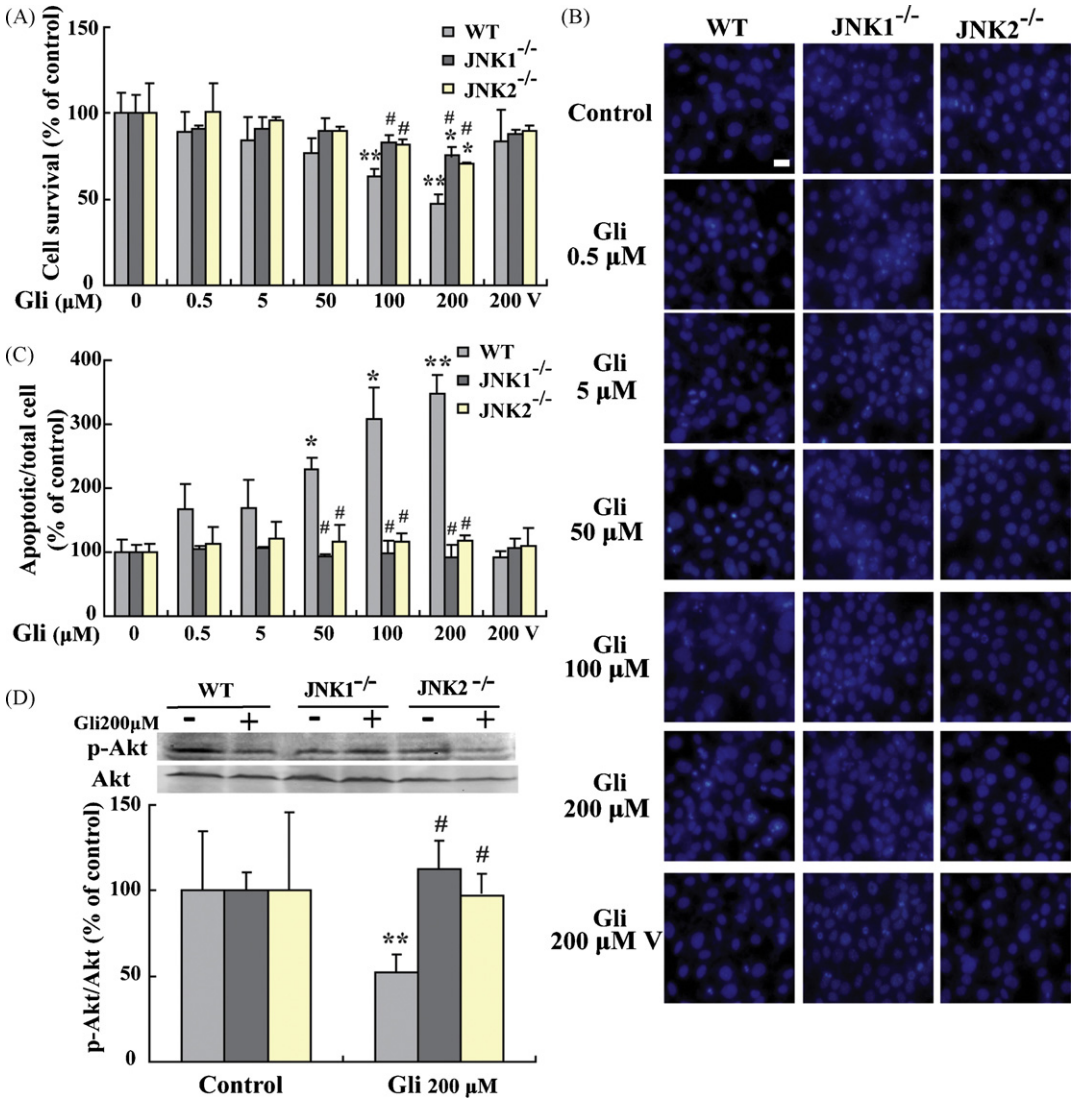

Fig. 5 – Effects of JNK on glibenclamide-induced anticancer activity. Wild-type and JNK1$^{-/-}$ or JNK2$^{-/-}$ MEF cells were treated with indicated concentration of glibenclamide for 48 h and then cellular viability and the apoptotic cells were detected with MTT assay (A) and fluorescence microscopy images of Hoechst 33342-stained cells (B), respectively. Scale bar: 50 μm. (C) Wild-type and JNK1$^{-/-}$ or JNK2$^{-/-}$ MEF cells were incubated with glibenclamide (200 μM) for 24 h, and then, cell proteins were obtained and analyzed with antiphospho-Akt and anti-Akt antibodies by Western blot. $^{*}P < 0.05$ vs. control group; $^{**}P < 0.01$ vs. control group; $^{\#}P < 0.05$ vs. WT group.

expression can enhance the activity of NADPH oxidase and subsequently the production of ROS [41]. The present study demonstrated that glibenclamide significantly increased gp91^{phox} expression and NADPH-oxidase-derived superoxide anion (O_2^-) generation, suggesting that glibenclamide could activate NADPH oxidase, and in turn promote ROS generation. On the other hand, glibenclamide at a higher concentration (100 μM) caused retardation of mitochondrial respiratory chain in MGC-803 cells, and further increased ROS production.

One of the major events during apoptosis is the depolarization of the mitochondrial membrane potential (ΔΨm), which induces the release of pro-apoptotic proteins cytochrome c and apoptosis inducing factor (AIF) from the mitochondrial intermembrane space [42]. It has been recognized that the release of cytochrome c or AIF from mitochondria is a key step in the initiation of caspase-dependent or caspase-independent apoptotic pathways [43]. Depolarization of ΔΨm was observed as early as 3 h after glibenclamide treatment, and preceded by the release of cytochrome c and AIF. These results suggest that glibenclamide may exert its anticancer effect by initiating both caspase-dependent and caspase-independent apoptotic pathways.

Intracellular ROS accumulation inactivates MAPK phosphatases (MKPs) by oxidation of their catalytic cysteine, which leads to sustained activation of JNK that plays a central role in ROS-mediated cell death [27]. Akt, also known as protein kinase B (PKB), is a serine/threonine protein kinase that plays a pivotal role in many physiological processes, including metabolism, development, cell cycle progression, migration and survival [44–47]. Akt can prevent cell apoptosis by the

phosphorylation and inactivation of pro-apoptotic factors such as Bad, caspase-9 and FH transcription factors [48], while JNK activation can inhibit Akt anti-apoptotic signaling pathway [33]. We revealed that glibenclamide treatment resulted in a significant activation of JNK, and this activation could be suppressed by the antioxidant NAC. These results indicate that glibenclamide may induce MGC-803 cell apoptosis by ROS-mediated activation of JNK. This hypothesis was further supported by the findings that glibenclamide greatly decreased the cellular viability, induced apoptosis, and significantly inhibited Akt anti-apoptotic signaling pathway in wild-type MEF cells but not in the JNK1$^{-/-}$ or JNK2$^{-/-}$ MEF cells. It has been demonstrated that phosphorylated JNK translocates from cytosol to mitochondria, where JNK triggers mitochondrial membrane depolarization, thereby facilitates the release of mitochondrial proapoptotic proteins to the cytosol [49]. Therefore, glibenclamide may trigger the mitochondrial apoptosis pathways by activating JNK pro-apoptotic signaling and inhibiting Akt anti-apoptotic signaling pathways.

In summary, we demonstrate for the first time that human gastric cancer cell line MGC-803 cells express the K_{ATP} channels composed of Kir6.2 and SUR1 subunits. K_{ATP} channel blocker glibenclamide induces apoptosis of MGC-803 cells, and the production of ROS is related to its antitumor activity. The constructed model of action (Fig. 6) illustrates that glibenclamide induced ROS generation through closing the K_{ATP} channels located in cellular or mitochondrial membrane, which activated the pro-apoptotic stress kinase JNK, inhibited the anti-apoptotic kinase Akt, and subsequently resulted in loss of $\Delta\Psi m$. The loss of $\Delta\Psi m$ increased the release of cytochrome c and AIF from mitochondria, and eventually triggered the caspase-dependent and caspase-independent apoptosis pathway. Taken together, our findings suggest that glibenclamide is a promising anticancer agent and the K_{ATP} channel expressed in cancer cells may be a potential target for developing antitumor agents.

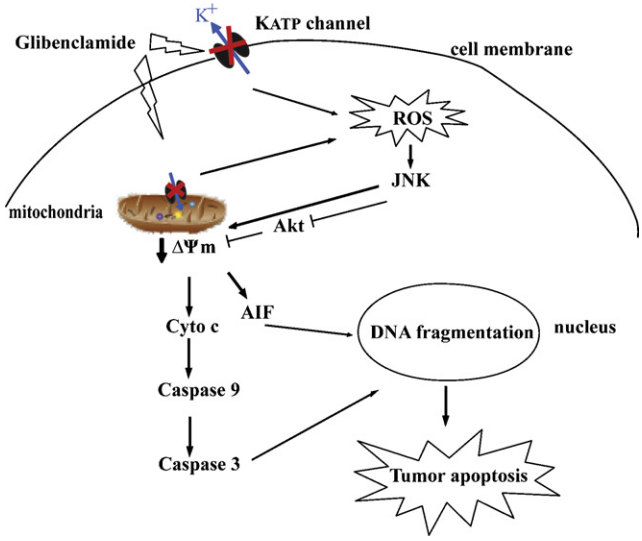

Fig. 6 – Schematic model for the mechanisms of glibenclamide-exerted antitumor activity. Glibenclamide-induced ROS generation activated the pro-apoptotic stress kinase JNK, inhibited the anti-apoptotic kinase Akt, and resulted in loss of $\Delta\Psi m$, which subsequently increased the release of cytochrome c and AIF from mitochondria, and eventually triggered the caspase-dependent and caspase-independent apoptosis pathway.

Acknowledgement

These studies were supported by grants from the National Natural Science Foundation of China (no. 30625038).

REFERENCES

[1] Miki T, Seino S. Roles of KATP channels as metabolic sensors in acute metabolic changes. J Mol Cell Cardiol 2005;38:917–25.
[2] Rodrigo GC, Standen NB. ATP-sensitive potassium channels. Curr Pharm Des 2005;11:1915–40.
[3] Ardehali H, O'Rourke B. Mitochondrial K(ATP) channels in cell survival and death. J Mol Cell Cardiol 2005;39:7–16.
[4] Busija DW, Lacza Z, Rajapakse N, Shimizu K, Kis B, Bari F, et al. Targeting mitochondrial ATP-sensitive potassium channels—a novel approach to neuroprotection. Brain Res Brain Res Rev 2004;46:282–94.
[5] Malhi H, Irani AN, Rajvanshi P, Suadicani SO, Spray DC, McDonald TV, et al. KATP channels regulate mitogenically induced proliferation in primary rat hepatocytes and human liver cell lines. Implications for liver growth control and potential therapeutic targeting. J Biol Chem 2000;275:26050–7.
[6] Wondergem R, Cregan M, Strickler L, Miller R, Suttles J. Membrane potassium channels and human bladder tumor cells: II. Growth properties. J Membr Biol 1998;161:257–62.
[7] Abdul M, Hoosein N. Expression and activity of potassium ion channels in human prostate cancer. Cancer Lett 2002;186:99–105.
[8] Valko M, Leibfritz D, Moncol J, Cronin MT, Mazur M, Telser J. Free radicals and antioxidants in normal physiological functions and human disease. Int J Biochem Cell Biol 2007;39:44–84.
[9] Alexandre J, Hu Y, Lu W, Pelicano H, Huang P. Novel action of paclitaxel against cancer cells: bystander effect mediated by reactive oxygen species. Cancer Res 2007;67:3512–7.
[10] Lambeth JD. NOX enzymes and the biology of reactive oxygen. Nat Rev Immunol 2004;4:181–9.
[11] Orrenius S, Gogvadze V, Zhivotovsky B. Mitochondrial oxidative stress: implications for cell death. Annu Rev Pharmacol Toxicol 2007;47:143–83.
[12] McCord JM. Human disease, free radicals, and the oxidant/antioxidant balance. Clin Biochem 1993;26:351–7.
[13] Kim HJ, Chakravarti N, Oridate N, Choe C, Claret FX, Lotan R. N-(4-Hydroxyphenyl)retinamide-induced apoptosis triggered by reactive oxygen species is mediated by activation of MAPKs in head and neck squamous carcinoma cells. Oncogene 2006;25:2785–94.
[14] Trachootham D, Zhou Y, Zhang H, Demizu Y, Chen Z, Pelicano H, et al. Selective killing of oncogenically transformed cells through a ROS-mediated mechanism by beta-phenylethyl isothiocyanate. Cancer Cell 2006;10:241–52.
[15] Feng R, Ni HM, Wang SY, Tourkova IL, Shurin MR, Harada H, et al. Cyanidin-3-rutinoside, a natural polyphenol antioxidant, selectively kills leukemic cells by induction of oxidative stress. J Biol Chem 2007;282:13468–76.

[16] Wang Y, He QY, Sun RW, Che CM, Chiu JF. GoldIII porphyrin 1a induced apoptosis by mitochondrial death pathways related to reactive oxygen species. Cancer Res 2005;65:11553–64.
[17] Fernandes DC, Wosniak Jr J, Pescatore LA, Bertoline MA, Liberman M, Laurindo FR, et al. Analysis of DHE-derived oxidation products by HPLC in the assessment of superoxide production and NADPH oxidase activity in vascular systems. Am J Physiol Cell Physiol 2007;292: C413–22.
[18] Ungvari Z, Csiszar A, Kaminski PM, Wolin MS, Koller A. Chronic high pressure-induced arterial oxidative stress: involvement of protein kinase C-dependent NAD(P)H oxidase and local renin-angiotensin system. Am J Pathol 2004;165:219–26.
[19] Gottlieb RA, Adachi S. Nitrogen cavitation for cell disruption to obtain mitochondria from cultured cells. Methods Enzymol 2000;322:213–21.
[20] Kruger NJ. The Bradford method for protein quantitation. Methods Mol Biol 1994;32:9–15.
[21] Lee SH, Doliba N, Osbakken M, Oz M, Mancini D. Improvement of myocardial mitochondrial function after hemodynamic support with left ventricular assist devices in patients with heart failure. J Thorac Cardiovasc Surg 1998;116:344–9.
[22] Tan S, Sagara Y, Liu Y, Maher P, Schubert D. The regulation of reactive oxygen species production during programmed cell death. J Cell Biol 1998;141:1423–32.
[23] Shimoni Y, Hunt D, Chuang M, Chen KY, Kargacin G, Severson DL. Modulation of potassium currents by angiotensin and oxidative stress in cardiac cells from the diabetic rat. J Physiol 2005;567:177–90.
[24] Zielonka J, Vasquez-Vivar J, Kalyanaraman B. Detection of 2-hydroxyethidium in cellular systems: a unique marker product of superoxide and hydroethidine. Nat Protoc 2008;3:8–21.
[25] Zhang S, Fu J, Zhou Z. In vitro effect of manganese chloride exposure on reactive oxygen species generation and respiratory chain complexes activities of mitochondria isolated from rat brain. Toxicol In Vitro 2004;18:71–7.
[26] Chandra J, Samali A, Orrenius S. Triggering and modulation of apoptosis by oxidative stress. Free Radic Biol Med 2000;29:323–33.
[27] Kamata H, Honda S, Maeda S, Chang L, Hirata H, Karin M. Reactive oxygen species promote TNFalpha-induced death and sustained JNK activation by inhibiting MAP kinase phosphatases. Cell 2005;120:649–61.
[28] Nakano H, Nakajima A, Sakon-Komazawa S, Piao JH, Xue X, Okumura K. Reactive oxygen species mediate crosstalk between NF-kappaB and JNK. Cell Death Differ 2006;13: 730–7.
[29] Antosiewicz J, Herman-Antosiewicz A, Marynowski SW, Singh SV. c-Jun NH(2)-terminal kinase signaling axis regulates diallyl trisulfide-induced generation of reactive oxygen species and cell cycle arrest in human prostate cancer cells. Cancer Res 2006;66:5379–86.
[30] Tournier C, Hess P, Yang DD, Xu J, Turner TK, Nimnual A, et al. Requirement of JNK for stress-induced activation of the cytochrome c-mediated death pathway. Science 2000;288:870–4.
[31] Sunters A, Madureira PA, Pomeranz KM, Aubert M, Brosens JJ, Cook SJ, et al. Paclitaxel-induced nuclear translocation of FOXO3a in breast cancer cells is mediated by c-Jun NH2-terminal kinase and Akt. Cancer Res 2006;66:212–20.
[32] Conti M. Targeting K+ channels for cancer therapy. J Exp Ther Oncol 2004;4:161–6.
[33] Wang H, Zhang Y, Cao L, Han H, Wang J, Yang B, et al. HERG K+ channel, a regulator of tumor cell apoptosis and proliferation. Cancer Res 2002;62:4843–8.
[34] Bonnet S, Archer SL, Allalunis-Turner J, Haromy A, Beaulieu C, Thompson R, et al. A mitochondria-K+ channel axis is suppressed in cancer and its normalization promotes apoptosis and inhibits cancer growth. Cancer Cell 2007;11:37–51.
[35] Bichet D, Haass FA, Jan LY. Merging functional studies with structures of inward-rectifier K(+) channels. Nat Rev Neurosci 2003;4:957–67.
[36] Nichols CG. KATP channels as molecular sensors of cellular metabolism. Nature 2006;440:470–6.
[37] Ashcroft FM. ATP-sensitive potassium channelopathies: focus on insulin secretion. J Clin Invest 2005;115:2047–58.
[38] Fang J, Nakamura H, Iyer AK. Tumor-targeted induction of oxystress for cancer therapy. J Drug Target 2007;15:475–86.
[39] Davies KJ. Oxidative stress: the paradox of aerobic life. Biochem Soc Symp 1995;61:1–31.
[40] Schumacker PT. Reactive oxygen species in cancer cells: live by the sword, die by the sword. Cancer Cell 2006;10:175–6.
[41] Rueckschloss U, Galle J, Holtz J, Zerkowski HR, Morawietz H. Induction of NAD(P)H oxidase by oxidized low-density lipoprotein in human endothelial cells: antioxidative potential of hydroxymethylglutaryl coenzyme A reductase inhibitor therapy. Circulation 2001;104:1767–72.
[42] Green DR, Reed JC. Mitochondria and apoptosis. Science 1998;281:1309–12.
[43] Saelens X, Festjens N, Vande Walle L, van Gurp M, van Loo G, Vandenabeele P. Toxic proteins released from mitochondria in cell death. Oncogene 2004;23:2861–74.
[44] Dummler B, Hemmings BA. Physiological roles of PKB/Akt isoforms in development and disease. Biochem Soc Trans 2007;35:231–5.
[45] New DC, Wong YH. Molecular mechanisms mediating the G protein-coupled receptor regulation of cell cycle progression. J Mol Signal 2007;2:2.
[46] Stambolic V, Woodgett JR. Functional distinctions of protein kinase B/Akt isoforms defined by their influence on cell migration. Trends Cell Biol 2006;16:461–6.
[47] Downward J. PI 3-kinase, Akt and cell survival. Semin Cell Dev Biol 2004;15:177–82.
[48] Vanhaesebroeck B, Alessi DR. The PI3K-PDK1 connection: more than just a road to PKB. Biochem J 2000;346(Pt 3): 561–76.
[49] Eminel S, Klettner A, Roemer L, Herdegen T, Waetzig V. JNK2 translocates to the mitochondria and mediates cytochrome c release in PC12 cells in response to 6-hydroxydopamine. J Biol Chem 2004;279:55385–92.